Molecular Cell, Volume *83*

Supplemental information

Implications of a multiscale structure of the yeast nuclear pore complex

Christopher W. Akey, Ignacia Echeverria, Christna Ouch, Ilona Nudelman, Yi Shi, Junjie Wang, Brian T. Chait, Andrej Sali, Javier Fernandez-Martinez, and Michael P. Rout

Supplemental Information

Implications of a multiscale structure of the yeast Nuclear Pore Complex

Christopher W. Akey, Ignacia Echeverria, Christna Ouch, Ilona Nudelman, Yi Shi, Junjie Wang, Brian T. Chait, Andrej Sali, Javier Fernandez-Martinez and Michael P. Rout

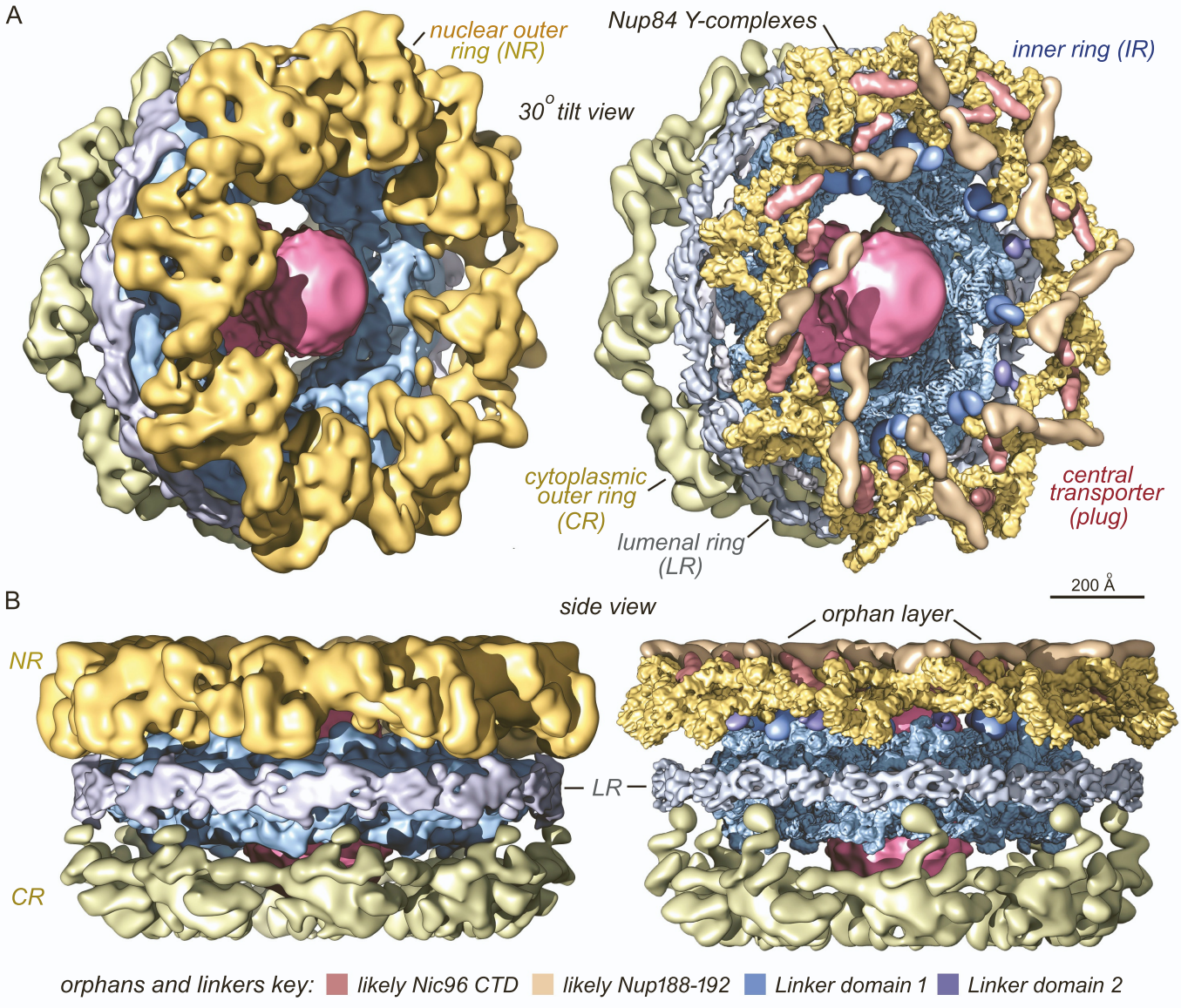

Figure S1. A step back is a step forward: composite structures of the yeast NPC are shown as isosurfaces with lower resolution 3D maps on the left and intermediate resolution maps on the right, related to FIgures 1, 2, 4, 5.

(A) NPC images are shown with a counter clockwise rotation of 30 degrees from a face-on, nuclear view.
(B) Composite structures viewed from the pore membrane. Individual rings and sub-assemblies are color coded as indicated in the key.

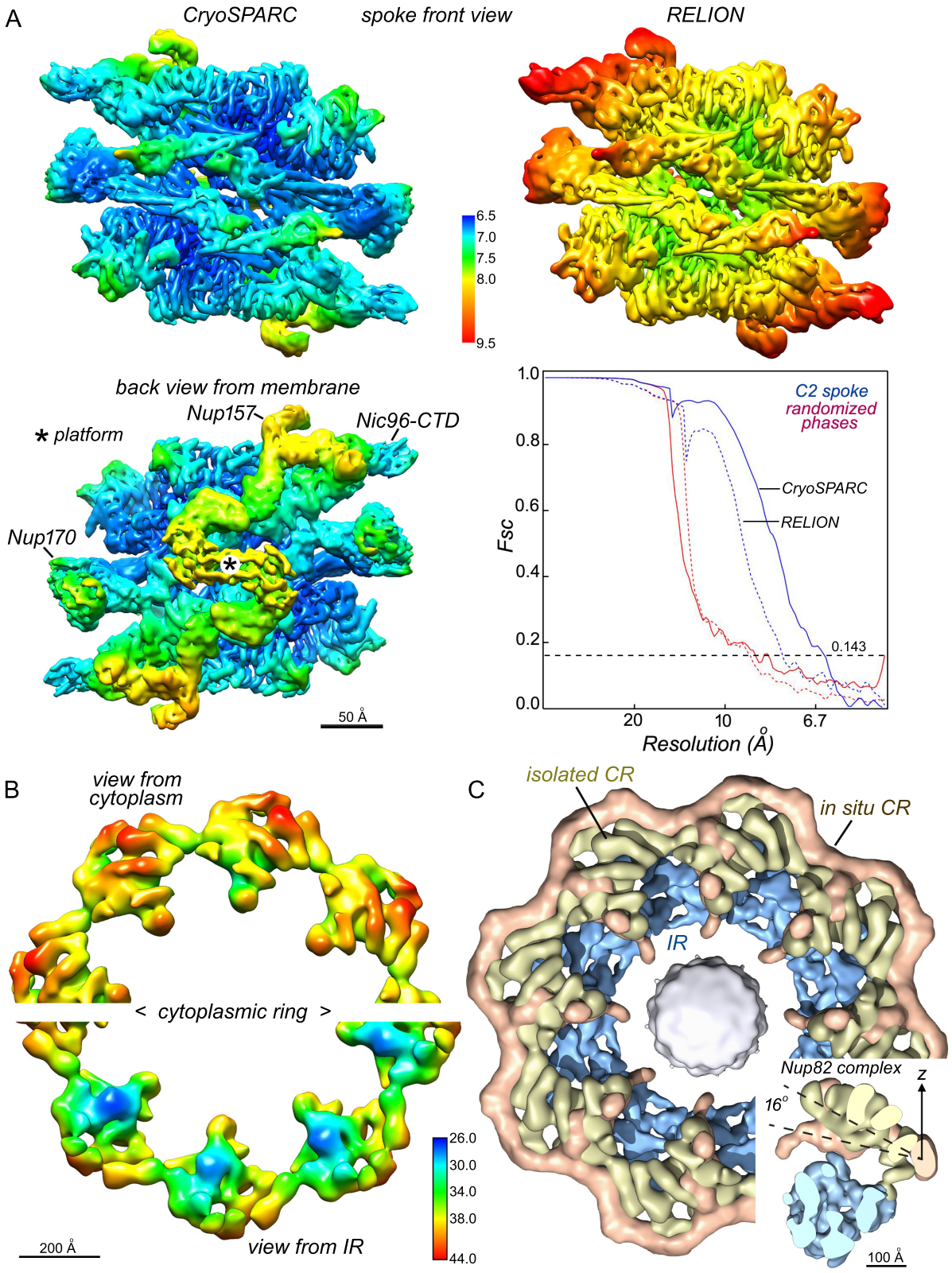
A
CryoSPARC
spoke front view
RELION
6.5
7.0
7.5
8.0
9.5
back view from membrane
Nup157
Nic96-CTD
* platform
Nup170
50 Å
C2 spoke
randomized
phases
CryoSPARC
RELION
Fsc
0.143
Resolution (Å)
B
view from
cytoplasm
< cytoplasmic ring >
26.0
30.0
34.0
38.0
44.0
200 Å
view from IR
C
isolated CR
in situ CR
IR
Nup82 complex
16°
z
100 Å

Figure S2. **Resolution of the spoke and characterization of the cytoplasmic outer ring, related to Figures 1, 2.**

(A) (top row) Local resolution maps for a single spoke. A side-by-side comparison is shown on the same resolution scale for 3D maps calculated in CryoSPARC (left) and RELION (right). (bottom row: left) A resolution gradient is present as the spoke approaches the micelle ring, whose position is indicated by an incomplete, platform-like feature (asterisk) for the Pom34-Pom152 TMDs. (bottom row: right) FSC curves for spoke maps.
(B) (top) Local resolution map for half of the cytoplasmic outer ring viewed from the cytoplasm. (bottom) A nuclear view with the half ring flipped by 180 degrees about the X-axis.
(C) The cytoplasmic outer ring from the isolated NPC (bronze) is ~15%. smaller in diameter than its *in situ* counterpart (shown in brown). Inset: Isolated and *in situ* cytoplasmic rings are viewed from the side to reveal a vertical rotation of the density for a Nup82 complex dimer.

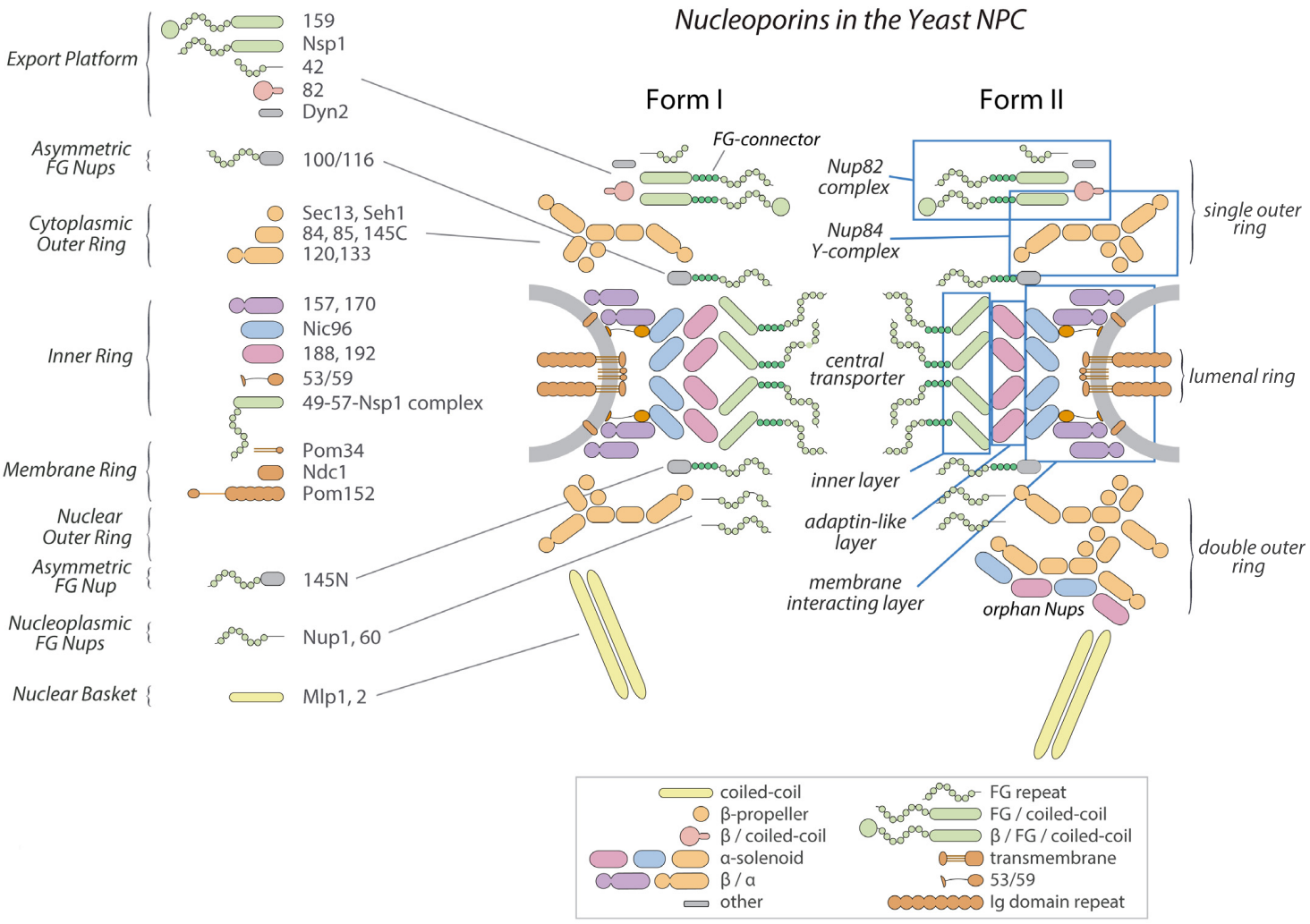

Figure S3. Diagram for Nups in Form I and Form II yeast NPCs, related to Figures 2, 4, 5.

FG-connectors are shown as a string of dark green circles that lead into the more flexible FG-repeats (light green). Individual sub-assemblies and functional regions are indicated in blue boxes and are labeled. Protein characteristics are categorized in the color coded key.

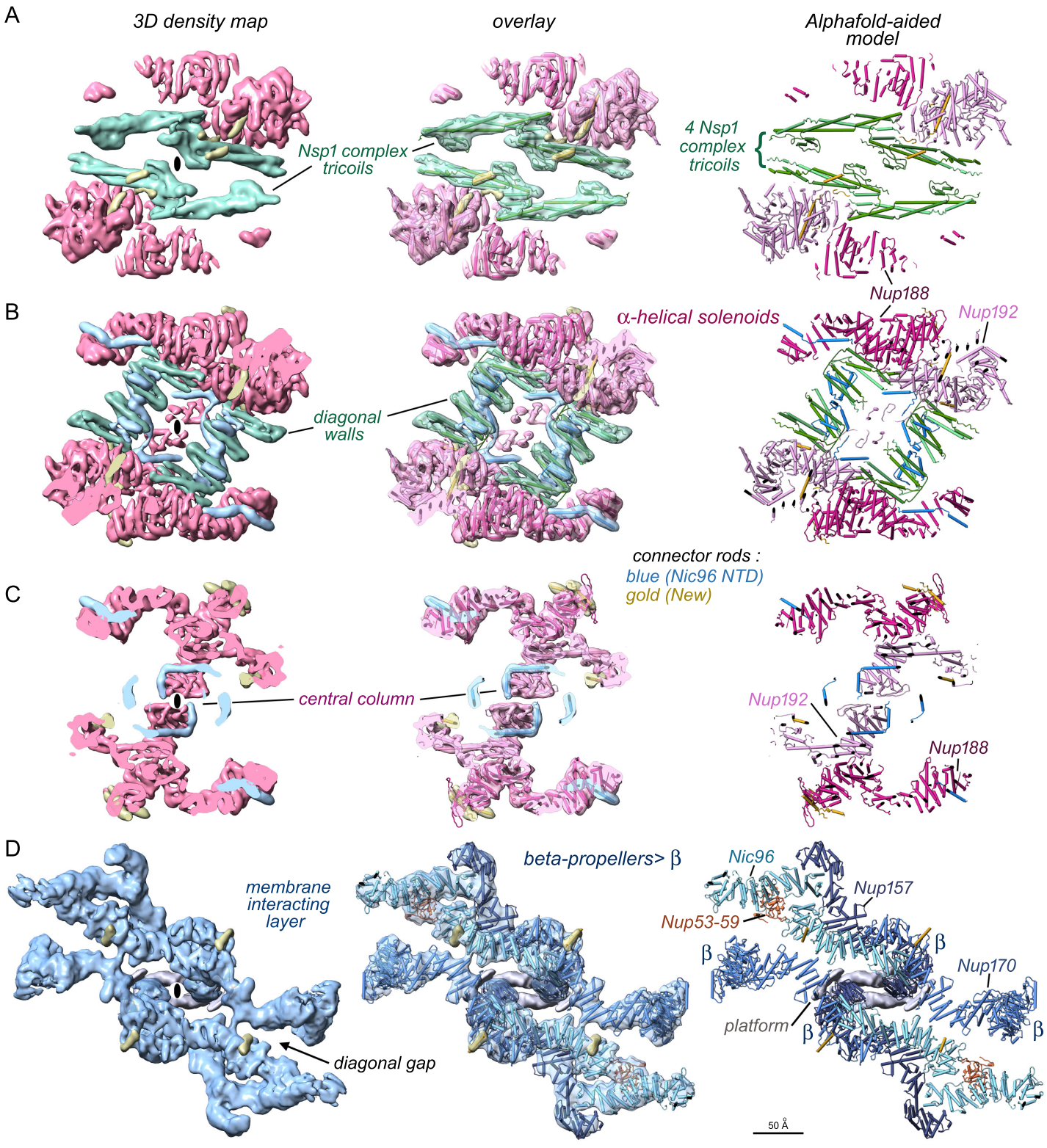
A
3D density map
overlay
Alphafold-aided model
Nsp1 complex tricoils
4 Nsp1 complex tricoils
Nup188
B
α-helical solenoids
Nup192
diagonal walls
connector rods :
blue (Nic96 NTD)
gold (New)
C
central column
Nup192
Nup188
D
membrane interacting layer
beta-propellers> β
Nic96
Nup157
Nup53-59
β
β
Nup170
platform
β
β
diagonal gap
50 Å

Figure S4. **Density map segmentation and docked models for Nups in three spoke layers, related to Figures 2,3.**

Sequential slabs are presented in each row starting from the central channel, while three columns provide different views for each slice including: an isosurface of the 3D density map, a semi-transparent view with docked Nups in cylinder and plank representation, and the molecular model. Nup color coding as in **Figure 2** including spoke connectors.

(A) Helical trimers of the Nsp1 complex (green) face into the central channel. The adaptin layer is in dark pink.
(B) Diagonal walls of α-helices formed by the Nsp1 complex with Nic96 connectors.
(C) A central column is formed by Nup192 CTD tails with bound Nic96 connectors.
(D) Membrane interacting layers of each half spoke are tilted and associate weakly along their lateral surfaces; they contain bound connectors and Nup53-Nup59 heterodimers (coral).

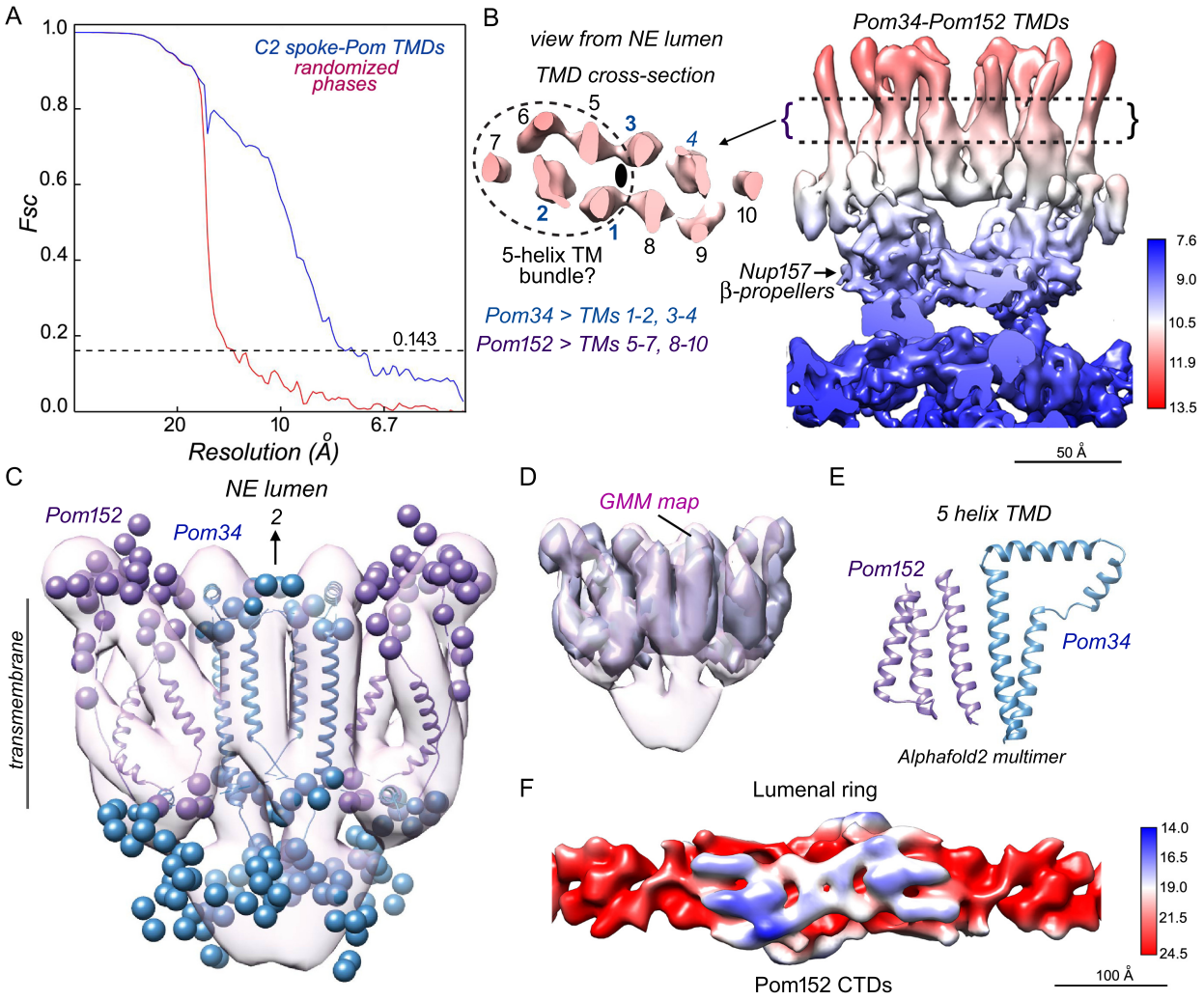

Figure S5. Characterization of Pom34 and Pom152 TMDs and the lumenal ring, related to Figure 4.

(A) FSC curves for the Pom34-Pom152 TMDs and a closely opposed region of the spoke with C2 symmetry after refinement in RELION.
(B) Orthogonal slice (on the left) and side view of the Pom34- Pom152 TMDs.
(C) Integrative structure model of the Pom34- Pom152 TMDs: the structural ensemble is presented as a 3D localization probability density whose surface is rendered transparent for visual clarity. Two-fold symmetry was applied to compute the model.
(D) Superposition of the model 3D localization probability density (purple, transparent) and the 3D GMM density map (solid).
(E) AlphaFold2-multimer prediction for the Pom34- Pom152 TMDs.
(F) Two repeats of the lumenal ring centered on the central spoke 2-fold axis and viewed from the NE lumen.

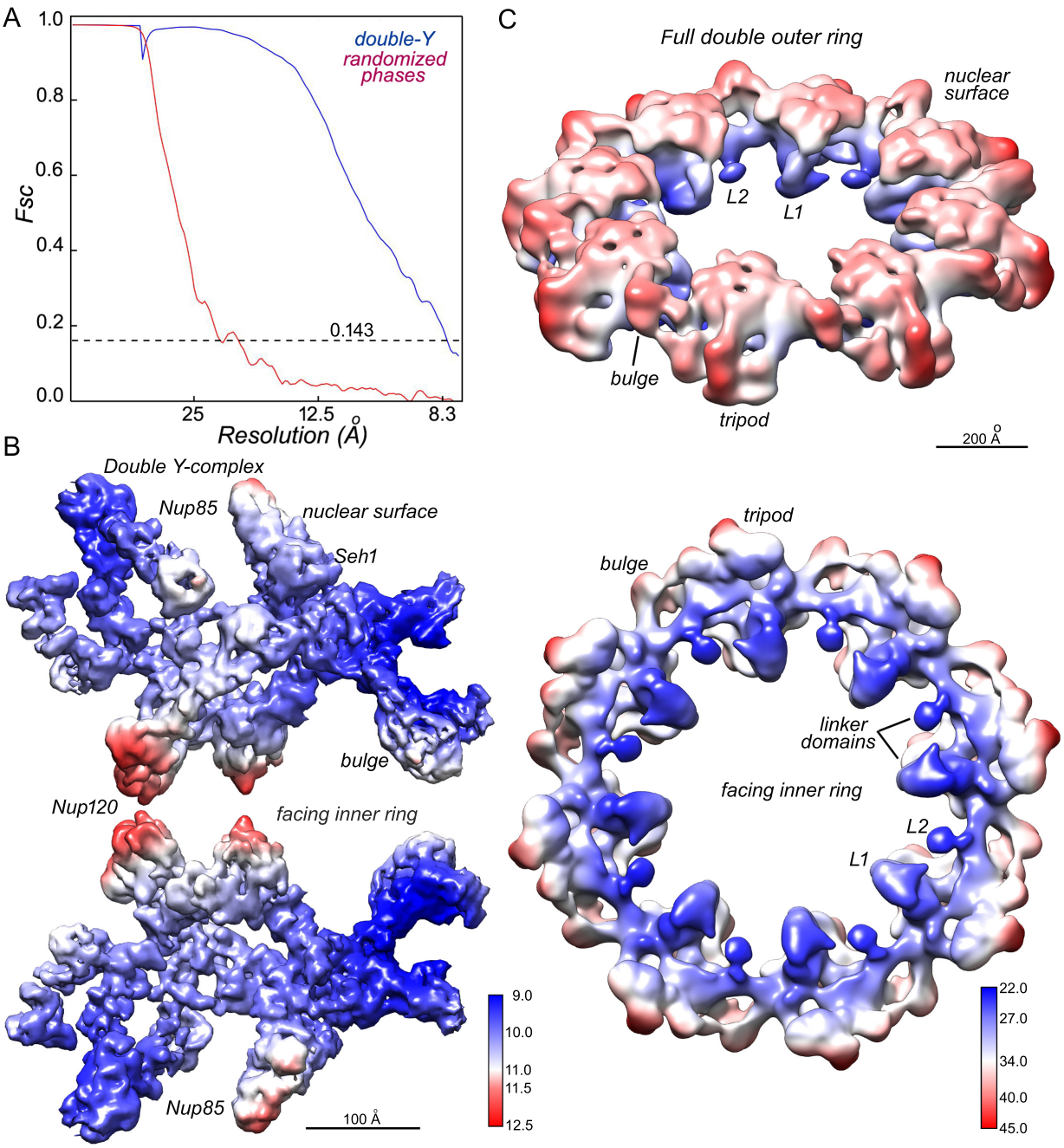

Figure S6. Resolution of double Y-complexes and full double outer ring, related to Figure 5.

(A) FSC plot for Nup84 double Y-complex protomer analyzed with CryoSPARC. Blue curve - masked FSC, Red curve - phase randomized and masked FSC.
(B) A local resolution 3D density map for the double Y-complex protomer with two views related by a 180 degree flip about the X-axis.
(C) (top) A tilted side view is shown for the local resolution 3D density map of the full double outer ring. (bottom) A view from the inner ring.

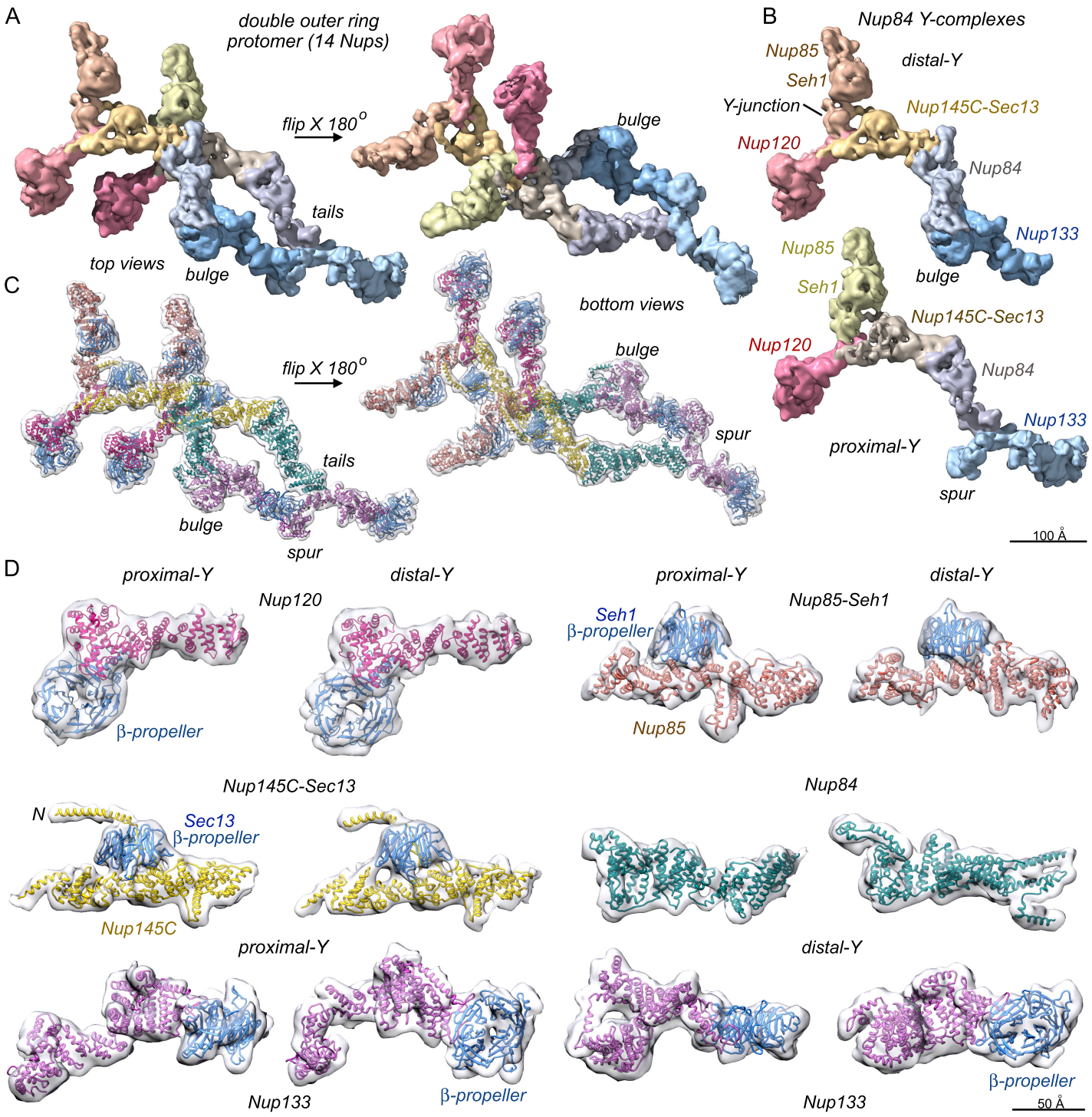
A
double outer ring
protomer (14 Nups)
flip X 180°
bulge
tails
top views
bulge
B
Nup84 Y-complexes
Nup85
Seh1
distal-Y
Y-junction
Nup145C-Sec13
Nup120
Nup84
Nup133
bulge
C
bottom views
flip X 180°
bulge
spur
tails
bulge
spur
Nup85
Seh1
Nup145C-Sec13
Nup120
Nup84
Nup133
proximal-Y
spur
100 Å
D
proximal-Y
distal-Y
Nup120
β-propeller
proximal-Y
distal-Y
Seh1
β-propeller
Nup85-Seh1
Nup85
Nup145C-Sec13
Nup84
N
Sec13
β-propeller
Nup145C
proximal-Y
distal-Y
Nup133
β-propeller
Nup133
β-propeller
50 Å

Figure S7. **Density map segmentation and model fitting for Nup84 Y-complexes in the nuclear double outer ring, related to Figure 5.**

(A) Segmented 3D density map for Nups in the double Y-complex. (left) View from the nucleus, (right) view from the inner ring.
(B) Single Nup84 Y-complexes are offset vertically from their relative positions in the protomer of double Y-complexes and are viewed from the nuclear interior. Individual Nups and notable features are labeled.
(C) Nearly complete models for Nup84 complexes in the double-Y protomer. Molecular ribbons are color-coded as in panel D.
(D) Individual 3D maps of Nups within the two Nup84 Y-complexes are shown with docked models. (Rows 1 and 2) Nups from the proximal and distal Y-complex are shown side by side. (Bottom row) Two distinctive views are shown for Nup133 from both the proximal and distal Y-complex.

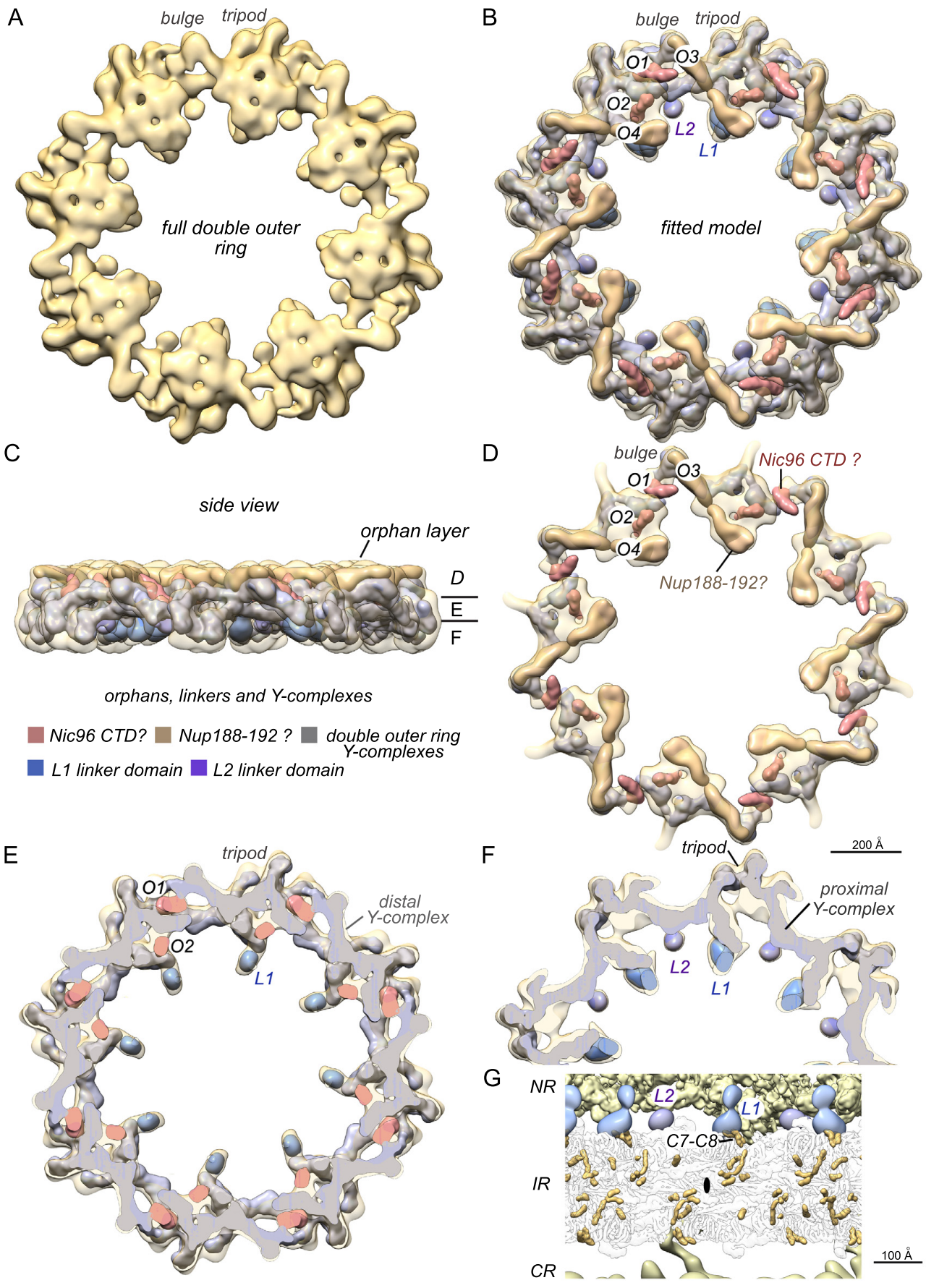
A
bulge
tripod
full double outer ring
B
bulge
tripod
O1
O3
O2
O4
L2
L1
fitted model
C
side view
orphan layer
D
E
F
orphans, linkers and Y-complexes
Nic96 CTD?
Nup188-192 ?
double outer ring Y-complexes
L1 linker domain
L2 linker domain
D
bulge
Nic96 CTD ?
O1
O3
O2
O4
Nup188-192?
E
tripod
O1
distal Y-complex
O2
L1
F
tripod
200 Å
proximal Y-complex
L2
L1
G
NR
L2
L1
C7-C8
IR
CR
100 Å

Figure S8. **Modeling the full double outer ring on the nuclear side of the yeast NPC, related to Figure 5.**

(A) Nuclear view of the full double outer ring refined with C8 symmetry.
(B) Fitted 3D model for the full double outer ring with color-coded components (see color key in panel C). Orphans (O1-O4) and linker domains (L1, L2) are labeled.
(C) Side view of the full double outer ring. The positions are indicated for thick slabs visualized in panels D, E and F.
(D) Top slab showing density features for the putative Nic96-CTD and Nup188-192 orphans, along with the double ring of Y-complexes (low pass filtered to 20Å resolution, in grey), docked in a transparent map of the full outer ring (in gold).
(E) Mid level slab showing fits for the double Y-complex, along with Nic96 CTDs and Linker domain 1.
(F) Half ring view of a density slab adjacent to the inner ring that contains the ring of double Y-complexes and both linker domains.
(G) The relationship between new connectors in the inner ring and the L1 linker domain is shown. Additional labels: nuclear double outer ring (NR), inner ring (IR) and cytoplasmic outer ring (CR).

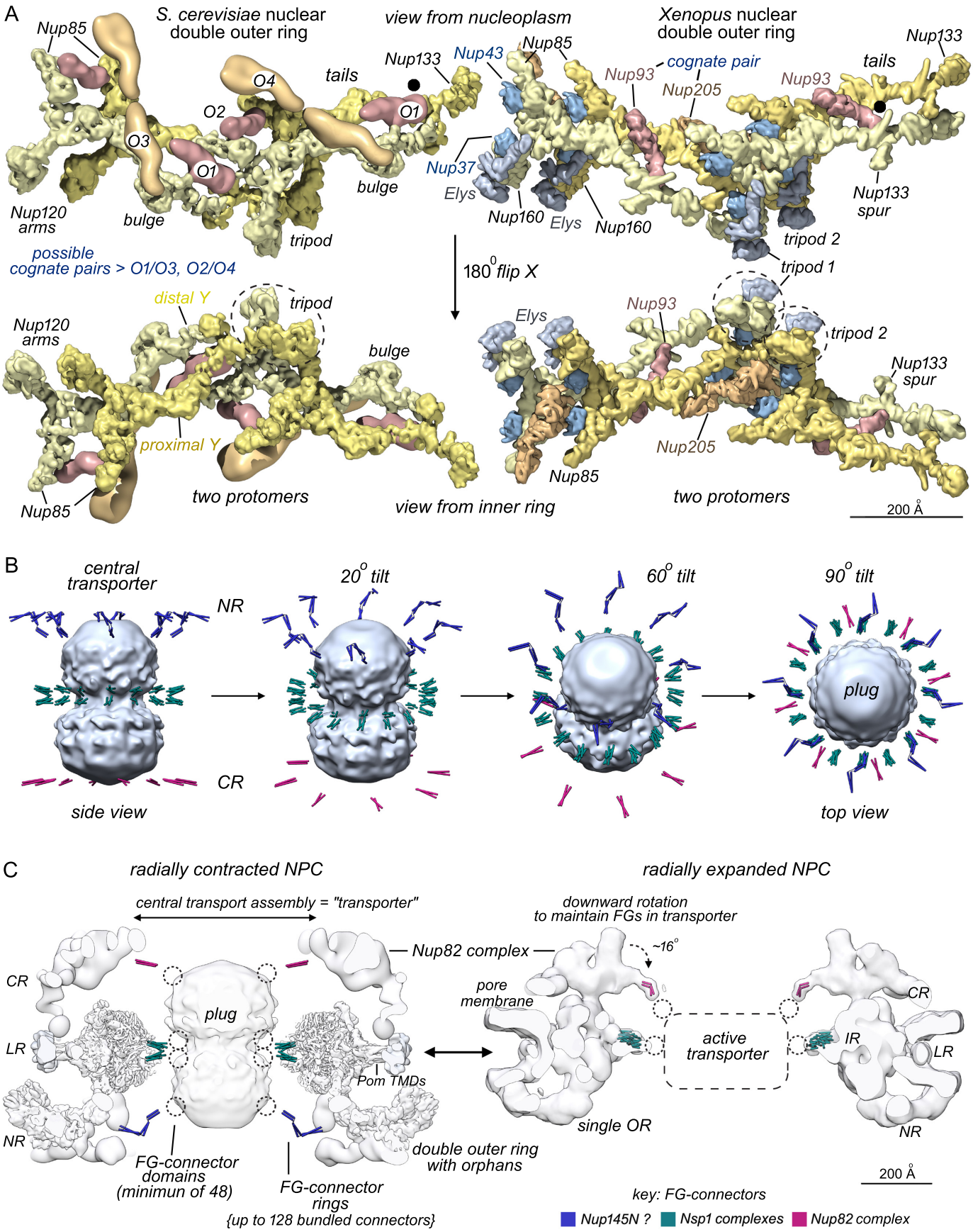
A
S. cerevisiae nuclear double outer ring
view from nucleoplasm
Xenopus nuclear double outer ring
Nup85
Nup133
Nup43
Nup85
cognate pair
Nup93
Nup205
Nup93
tails
tails
O4
O2
O1
O3
O1
Nup37
Elys
Nup160
Elys
Nup160
bulge
bulge
Nup120 arms
tripod
Nup133 spur
tripod 2
possible cognate pairs > O1/O3, O2/O4
180° flip X
tripod 1
distal Y
tripod
Nup120 arms
Elys
Nup93
tripod 2
bulge
Nup133 spur
proximal Y
Nup205
Nup85
Nup85
two protomers
view from inner ring
two protomers
200 Å
B
central transporter
NR
20° tilt
60° tilt
90° tilt
CR
plug
side view
top view
C
radially contracted NPC
radially expanded NPC
central transport assembly = "transporter"
downward rotation to maintain FGs in transporter
Nup82 complex
~16°
CR
pore membrane
plug
LR
active transporter
IR
CR
LR
Pom TMDs
NR
single OR
NR
FG-connector domains (minimun of 48)
FG-connector rings
{up to 128 bundled connectors}
double outer ring with orphans
200 Å
key: FG-connectors
Nup145N ?
Nsp1 complexes
Nup82 complex

Figure S9. Configuration of double Y-complex protomers and distribution of FG-connectors in the central channel of the NPC, related to Figures 5,6,7.

(A)(left) Y-complexes in two protomers from the nuclear double outer ring of yeast NPCs are shown as segmented 3D maps with associated orphans that may arise from cognate Nic96/ Nup188-192 pairs. A single tripod membrane binding site is formed at the interface between protomers (8 per double ring). (right) Two protomers from the nuclear double outer ring of *Xenopus* NPCs (7WB4.pdb)[32] are represented as smoothed 3D maps. Two closely-spaced, membrane binding tripods are formed at the interface between adjacent protomers with 16 tripods per double ring. Each β-propeller in a tripod contains an MBM to interact with the NE.
(B) A rotation series is shown for the central transporter/plug with associated FG-connectors (color key in **Figure 6C**).
(C) (left) Central cross-section of the composite model of a radially-contracted, Form II yeast NPC with color coded FG-connector rods. (right) Cross-section from a 3D density map of the Form I yeast NPC imaged *in situ* (EMD 24258)[7] with a diagram of the central transporter (dashed box) based on channel density from a 3D map of the *in situ* human NPC [21].

Table S1. Single particle data processing and modeling of the yeast NPC and sub-assemblies, related to FIgures 1-6.

Data collection	Single particle analysis	
Microscope	Titan-Krios-GIF	
Detector/Energy Filter Slit	K2 Summit/20e	
Image mode	Super-resolution counting	
Frames	40	
Total electron dose (e^-/ Å^2)	40.0	
Nominal pixel size (Å)	2.66	
Defocus range (μm)	1.5 to -3.8	
Movies (after triage)	4015 (3218)	
NPCs/protomers after cleaning	26049 /208392	
Sub-assembly	**Spoke (inner ring protomer)**	**Nuclear outer ring (Double-Y protomer)**
3D reconstruction	Multibody	Multibody
Symmetry imposed	C1 (C2 post)	C1
Software	RELION 3.0.7 and CryoSPARC	RELION 3.0.7 and CryoSPARC
final protomers	208392	29655
Nominal pixel size (Å)	2.66	3.99
Map resolution (Å) -masked FSC 0.143	6.6	8.1
Local resolution range (Å)	6.5-9.5	9-12.5
B-factor (Å^2)	-300	-600 (ad hoc)
Modeling		
Software-	Chimera, Coot, MDFF	Chimera, Coot, MDFF
NPC component Ordered mass	Full spoke	N-ring: double Y-complex
(MDa) /protomer	1.89	1.02
Number of Nucleoporins	28	14
Chimera map cross-correlation	0.9	0.84
EMDB/RCSB codes†	EMD-41300 / PDB 8TJ5	EMD-41285 / PDB 8TIE

Table S1 continued

	Additional sub-assembly maps				
Sub-assembly	**Pom34-Pom152 anchors**	**Bridges to central transporter (full NPC maps)**	**Lumenal ring**	**Full double outer ring**	**single outer ring**
details	**membrane attachment site**	**cytoplasmic Map 1 / nuclear Map 2**	**Map 1 / Map 2**	**nuclear side**	**cytoplasmic side**
3D reconstruction	Multibody and focused refinement	Global refinement after 3D classification	Multibody	Global refinement	Focused global refinement and Multibody
Symmetry imposed	C1 (C2 post)	C8/C8	C1 (C2 post)/ D8, C1 (C2 post)	C8	C8 / C1
Software	RELION 3.0.7	RELION 3.0.7	RELION 3.0.7	RELION 3.0.7	RELION 3.0.7
final protomers	208392	41120/11304	85322 / 341952	41120	41120 / 34576
Nominal pixel size (Å)	2.66	5.32 / 3.99	5.32	3.99	3.99
Map resolution (Å)- masked FSC 0.143	9.4	31.4 / 29.5	14.7/ ~20	23.0	30 / 22
Resolution range (Å)	10.5-12 (Pom/TMDs)	37-43 / 35-43	14-24 / 22-25	23-39	2-44 / 22-38
B-factor ($Å^2$)	-800	-1000 / -1000	-300 /-1000	-1000	-1000 / -1000
EMDB/RCSB codes†	EMD-41117 / PDB 8T9L	EMD-41122 / EMD-41121	EMD-41116	EMD-41114	EMD-41119

†Composite, multiscale 3D density maps for the yeast NPC (EMD-41123) and density map for the NPC with central transporter-plug (EMD-41120).

Table S2. Modeling the inner ring spoke and double Y-complex in the nuclear outer ring of the yeast NPC, related to Figures 2, 5.

Components	*PDB/Alphafold models (residues)*	*Maps & Template PDBs*
Spoke (inner ring)	28 Nucleoporins	EMD-24232 / 7N85
Nsp1 complexes (4 copies)	PDB 7N85	
Nup53/59 heterodimer (2)	PDB 7N85	
Nic96 NTD (4)	PDB 7N85 (15-166, 15-173)	
Nic96 CTD (4)	AF_AFP34077F1 (190-839, 198-839)	
Nup157 (2)	AF_AFP40064F1 (78-1391)	
Nup170 (2)	AF_AFP38181F1 (81-1326)	
Nup188 (2)	AF_AFP52593F1 (15-1655)	
Nup192 (2)	AF_AFP47054F1 (1-1683)	
Total residues modeled New/ previous (7N85.pdb)	17536 / 15584	
Structural features : New/previous (7N85.pdb)	α-helices 744/611 :: β-propellers 4/4 connectors 18†/28 total: 46	
Double Y-complex (outer ring)	14 Nucleoporins	EMD-24231 / 7N84
Nup120 (2 copies)	AF_AFP35729F1 (1-1037)	4XMM (Y-junction)
Nup85 (2)	AF_AFP46673F1 (66-744)	3EWE, 4XMM (Y-junction)
Seh1 (2)	AF_AFP53011F1 (1-349)	3EWE
Nup145C (2)	AF_AFP49687F1 (102-711, 113-711)	3JRO, 4XMM (Y-junction)
Sec13 (2)	AF_AFQ04491F1 (8-293)	3JRO
Nup84 (2)	AF_AFP52891F1 (1-726)	3JRO
Nup133 (2)	AF_AFP36161F1 (1-1157)	
Total residues modeled New/ previous (7N84.pdb)	9479 / 9092	
Structural features New/previous (7N84.pdb)	α-helices 341/324 :: β-propellers 8/8	
Totals	α-helices 1085 :: β-propellers 12 residues 27015/protomer :: mass 2.92 MDa (no cytoplasmic outer ring, TMDs or lumenal ring)	

† At the current resolution, most new connectors modeled as helices with a few strands but higher resolution is needed to identify their secondary structure.

References:

3EWE : Brohawn, S.G., Leksa, N.C., Spear, E.D., Rajashankar, K.R., Schwartz, T.U. (2008) Science 322**:** 1369-1373.

3JRO : Brohawn, S.G., Schwartz, T.U. (2009) Nat Struct Mol Biol 16**:** 1173-1177.

4XMM : Stuwe, T., Correia, A.R., Lin, D.H., Paduch, M., Lu, V.T., Kossiakoff, A.A., Hoelz, A. (2015) Science 347: 1148-1152.

Alphafold models: Jumper, J. et al. (2021). Highly accurate protein structure prediction with AlphaFold. Nature 596: 583–589.

Table S3. Orphan spoke connectors from Nup145N and Nup53 in a half spoke, related to Figure 3.

connector	partner	identity	PDB and comments
C1	Nup57-Nsp1	unknown	~15 residue α-helix and extended chain faces into central channel
C2	Nsp1-Nup57	unknown	~13 residue extended chain
C3	Nup192-NTD	Nup145N	7MVV : displaced 11 extended residues
C4	Nup192-NTD	unknown	~35 residue α-helix in crook of Nup192-NTD
C5	Nup192-NTD-Nup57	unknown	~17 residues
C6	Nup170 α-helical solenoid	Nup145N	5HB0 : ~25 residue bent α-helix
C7	Nup188	Nup145N	7MVZ: ~22 reside α-helix and extended chain Adjacent to SH3-like domain in Nup188
C8	Nup188	Likely Nup145N	~37 residues in bent α-helix, adjacent to C6 Adjacent to SH3-like domain in Nup188
C9	Nic96-CTD innermost copy	Nup53	5HB3: ~17 reside α-helix

Table S4. Summary of the Pom34-Pom152 tetramer integrative structure modeling, related to Figure 4.

1) Gathering information	2-fold symmetry derived from cryo-EM structure
Prior models	Excluded volume
Physical principles and statistical preferences	Sequence connectivity 14 DSS0
Experimental data	Atomic structure prediction from Alphafold2 (AF _Q12445, AF _P39685)
2) Representing the system	
Composition (number of copies)	4
Atomic (structured) components	Pom152: 105-130, 144-167, 176-192, 200-212, 105-130, 144-167, 176-192, 200-212 Pom34: 44-86, 89-110, 122-150, 222-237, 44-86, 89-110, 122-150, 222-237
Unstructured components	Pom152: 1-104, 131-143, 168-175, 193-199, 213-250, 1-104, 131-143, 168-175, 193-199, 213-250 Pom34: 1-43, 87-88, 111-121, 151-221, 238-250, 1-43, 87-88, 111-121, 151-221, 238-250
Resolution of structured components	1 [R1] residue per bead
Resolution of unstructured components	2 [R2] residues per bead
Structural coverage	37.76 %
Rigid body (RB) definitions	RB1: Pom152 $_{105-130}$ RB2: Pom152 $_{144-167}$ RB3: Pom152 $_{176-192}$ RB4: Pom152 $_{200-212}$ RB5: Pom34 $_{44-86}$ RB6: Pom34 $_{89-110}$
Resolution of disordered regions	2 [R2] residues per bead
Spatial restraints encoded into scoring function	Excluded volume; applied to the R1 representation Sequence connectivity; applied to the R1 representation Cross-link restraints; applied to the R1 representation
3) Structural Sampling	
Sampling method	Replica Exchange Gibbs sampling, based on Metropolis Monte Carlo
Replica exchange temperature range	1.0 - 4.0
Number of replicas	6
Number of runs	80
Number of structures generated	6400000

Table S4 continued

Movers for flexible string of bead	Random translation up to 4.0 Å
CPU time	22 hours on 80 processors
4) Validating the Pom34-Pom152 models	
Models selected for validation	
Number of models after equilibration	6400000
Number of models that satisfy the input information	7089
Number of structures in samples A/B	2378/4711
p-value of non-parametric Kolmogorov-Smirnov two-sample test	0.539 (threshold p-value > 0.05)
Kolmogorov-Smirnov two-sample test statistic, D	0.0
Thoroughness of the structural sampling	
Sampling precision	14.08 Å
Homogeneity of proportions χ^2 test (p-value)/Cramers V value	1.000/0.000 (thresholds: p-value > 0.05 OR Cramer's V < 0.1)
Number of clusters	1
Cluster populations	cluster 1 : 100.0 %
Cluster precisions	cluster 1 : 9.52 Å
Average cross-correlation between localization probability densities of samples A and B	cluster 1: 0.78
Validation by information used for modeling	
Percent of sequence connectivity restraints satisfied per structure	99 %
Percent cross-link restraints satisfied by ensemble	99 %
Percent of excluded volume restraints satisfied per structure	99 %
5) Software and data availability	
Software	
Modeling programs	IMP PMI module, version develop-1350fc67f7 Integrative Modeling Platform (IMP), version develop-1350fc67f7
Modeling scripts	https://github.com/integrativemodeling/NPC-TMD
Structure prediction	AlphaFold2
Visualization and plotting Data	UCSF Chimera
Data deposition PDBDEV_00000213	

Table S5. Notable orphans, linkers and lateral contacts in the yeast double outer ring, related to Figure 5.

Components	*Partners*	*Comments*
Orphans		
Nup188-192 (O3)	distal Nup145C/Nup84	May stabilize distal Nup84 Y-complex
Nic96CTD (O1)	distal Nup133/ proximal Nup84	Located between tails in double-Y
Nup188-192 (O4)	Nup188-192/linker 1	Orient linker 1 ?
Nic96CTD (O2)	proximal Nup85/ distal Seh1	Located between two Nup85 arms
Linker domains		
Linker 1	Nup188-192(O4)-proximal Nup85 to Nup188 (IR)	Links double ring to inner ring, sits above SH3-like domain in Nup188 of the spoke
Linker 2	proximal Nup145C/Nup84 to Nup53/Nup59 (IR)	Links double ring to inner ring
Contacts		
Intra Y-complex contacts in the protomer	(amino acid residues)	
distal Nup145C (112-124)	distal Nup85 (621-623)	Connects Y-stem to Nup84 arm
proximal Nup145C (102-112)	proximal Nup85 (622-623)	Connects Y-stem to Nup84 arm
distal Nup84 (406-726)	distal Nup133 (705-1157)	Forms novel bulge in distal Y-complex
Inter Y-complex contacts In the protomer		
distal Nup133 beta propeller (51-482)	proximal Nup133 spur (941-1157)	Major contact between adjacent tails in double Y-complex
Contacts between double Y-complexes in the outer ring		
proximal Nup133 helical solenoid and beta propeller (multiple sites)	proximal and distal Nup120	Major double Y complex contact sites in ring Tripod membrane interaction site
proximal Nup84 (610-612)	distal Nup85 (601-616)	Align Nup85 arm
proximal Nup84 (51-63)	distal Nup85 (295-302)	Align Nup85 arm

Figure S6. Nucleoporin FG repeats in the central transport channel of the yeast NPC, related to Figures 6,7.

Nucleoporins/NPC from C- to N-side (number of copies)	FG repeat residues	Total amino acids	Mass for FG repeats approximate
Nup42 (8)	364	2912	0.28×10^6
Nsp1 (16)	590	9440	1.00×10^6
Nup159 (16)	876	14016	1.51×10^6
Nup116 (16)	686	10976	1.18×10^6
Nup100 (16)	570	9120	0.98×10^6
			~4.9 MDa
Nsp1 (32)	590	18880	2.00×10^6
Nup49 (32)	236	7522	0.81×10^6
Nup57 (32)	220	7040	0.76×10^6
			~3.6 MDa
Nup145N (16)	209	3344	0.36×10^6
Nup1 (8)	695	5560	0.6×10^6
Nup60 (8)	~100	800	0.09×10^6
			~1.1 MDa
		Sum	~9.6 MDa